Junlian Gu,[1,2,3] Yanli Cheng,[1,2,3] Hao Wu,[3,4] Lili Kong,[1,3] Shudong Wang,[1,3]
Zheng Xu,[1,3] Zhiguo Zhang,[1] Yi Tan,[2,3,5] Bradley B. Keller,[3,6] Honglan Zhou,[1]
Yuehui Wang,[1] Zhonggao Xu,[1] and Lu Cai[1,2,3,5]

Metallothionein Is Downstream of Nrf2 and Partially Mediates Sulforaphane Prevention of Diabetic Cardiomyopathy

We have reported that sulforaphane (SFN) prevented diabetic cardiomyopathy in both type 1 and type 2 diabetes (T2DM) animal models via the upregulation of nuclear transcription factor erythroid 2–related factor 2 (Nrf2) and metallothionein (MT). In this study, we tested whether SFN protects the heart from T2DM directly through Nrf2, MT, or both. Using Nrf2-knockout (KO), MT-KO, and wild-type (WT) mice, T2DM was induced by feeding a high-fat diet for 3 months followed by a small dose of streptozotocin. Age-matched controls were given a normal diet. Both T2DM and control mice were then treated with or without SFN for 4 months by continually feeding a high-fat or normal diet. SFN prevented diabetes-induced cardiac dysfunction as well as diabetes-associated cardiac oxidative damage, inflammation, fibrosis, and hypertrophy, with increases in Nrf2 and MT expressions in the WT mice. Both Nrf2-KO and MT-KO diabetic mice exhibited greater cardiac damage than WT diabetic mice. SFN did not provide cardiac protection in Nrf2-KO mice, but partially or completely protected the heart from diabetes in MT-KO mice. SFN did not induce MT expression in Nrf2-KO mice, but stimulated Nrf2 function in MT-KO mice. These results suggest that Nrf2 plays the indispensable role for SFN cardiac protection from T2DM with significant induction of MT and other antioxidants. MT expression induced by SFN is Nrf2 dependent, but is not indispensable for SFN-induced cardiac protection from T2DM.

Diabetic cardiomyopathy (DCM) is a major cause of the mortality in patients with diabetes (1,2); however, there remains no effective preventive approach. Given that reactive oxygen species has been considered to be a critical mechanism for the development of DCM (3,4), antioxidant therapy has obtained more attention.

Nuclear transcription factor erythroid 2–related factor 2 (Nrf2) plays an important role in antioxidative responses by upregulating multiple antioxidant components such as heme oxygenase-1 (HO-1) and NAD(P)H:quinone oxidoreductase 1 (NQO1) (1,5). Sulforaphane (SFN) is a potent Nrf2 activator. We have reported that SFN upregulates Nrf2 function and protects from DCM in mice with type 1 diabetes (T1DM) induced by streptozotocin (STZ) (6) and mice with type 2 diabetes (T2DM) induced by feeding a high-fat diet (HFD) followed by small dose of STZ (HFD/STZ) (7). Silencing the *Nrf2* gene in cultured H9c2 cardiac cells abolished SFN's prevention of high-level glucose–induced cellular oxidative damage (6). However, whether Nrf2 really plays an indispensable role in the prevention of DCM by SFN remains unclear.

In addition, because Nrf2 is a nuclear transcription factor, Nrf2 itself does not have antioxidant function, and its antioxidant effect has to be mediated by downstream targets. Metallothionein (MT) is a cysteine-rich and metal-binding protein (8) and has been shown to protect the heart from T1DM and T2DM in mouse models (8–10). Induction of MT expression by zinc administration for 3 months almost completely prevented DCM (9), but only partially prevented diabetic nephropathy (11), suggesting different contributions

of MT protection from oxidative damage in diabetes to the heart and kidney.

Reportedly, SFN induces MT expression in vitro (12) and in vivo (13). We also demonstrated the significant SFN induction of MT mRNA expression in the heart of T1DM mice (6) and the kidney of T2DM mice (2). Furthermore, we found that MT plays an important role in SFN-mediated Nrf2 renal protection (2). However, whether MT also plays an important role in SFN-mediated protection against DCM in T1DM or T2DM model has not been determined.

In the current study, therefore, we explored whether Nrf2 plays the requisite role in SFN-mediated protection from DCM in the T2DM model and, if so, whether MT acts as one of the Nrf2 downstream genes to play a critical role in SFN-induced Nrf2-mediated protection from DCM. The combination of Nrf2-knockout (KO), MT-KO, and wild-type (WT; C57BL/6J or 129S1) mice was used for inducing a T2DM model with HFD/STZ (7).

RESEARCH DESIGN AND METHODS

Animals and Experimental Models

Eight-week-old male Nrf2-KO mice were obtained by breeding homozygotes (Nrf2$^{-/-}$) with heterozygotes (Nrf2$^{+/-}$), and MT-KO mice were obtained from breeding homozygotes (MT$^{-/-}$) with heterozygotes (MT$^{+/-}$). All breeding pair mice were purchased from The Jackson Laboratory (Bar Harbor, ME). All experimental procedures were approved by the Institutional Animal Care and Use Committee of the University of Louisville.

T2DM features two physiological defects: resistance to the action of insulin combined with deficient insulin secretion (7,14). Accordingly, an insulin-defective T2DM mouse model was created by HFD feeding for 3 months to induce insulin resistance (Supplementary Fig. 1A), followed by a single dose of STZ to cause mild deficiency of insulin secretion and hyperglycemia, as illustrated in Supplementary Fig. 1B and previously described (7,14). The HFD contains 60% kcal fat (no. 12492; Research Diets, New Brunswick, NJ), and the control normal diet (ND) contains 10% kcal fat (no. 12450B; Research Diets). The STZ was given by a single intraperitoneal injection of 100 mg/kg in 0.1 mol/L sodium citrate buffer (pH 4.5; Sigma-Aldrich, St. Louis, MO) (7). Five days after STZ administration, HFD/STZ mice with hyperglycemia (3-h fasting blood glucose levels ≥250 mg/dL) were considered as IDS-T2DM. Then, both T2DM and control mice were injected subcutaneously with or without SFN (Sigma-Aldrich) at 0.5 mg/kg 5 days a week for 4 months along with continual feeding with either HFD or ND. Accordingly, four groups were defined: ND + vehicle (Ctrl), ND + SFN (SFN), HFD/STZ + vehicle (DM), and DM + SFN (DM/SFN).

The selection of an SFN dose of 0.5 mg/kg was based on the following considerations: 1) because of its lipophilicity, SFN is rapidly absorbed entirely, and the plasma concentration appears at ~1 h and peaks at 4 h after dosing, with a half-life of 2.2–2.6 h in rats and humans (13,15,16); and 2) SFN is rapidly excreted. Therefore, doses

of SFN at 10-fold difference reached the similar levels of plasma concentrations of SFN and half-life time (16). This may be the reason why a wide range of SFN dosing, 40 μg to 25 mg/kg, has been used in animal models (17). Due the chronic treatment experimental design, we used a relatively low (0.5 mg/kg daily of the working day) for relative long time (4 months), which has been shown to have limited unanticipated side effects (6,7,18,19).

Echocardiography

Transthoracic echocardiography was performed to measure cardiac function (7). Briefly, we used a high-resolution imaging system (Vevo 770; Visual Sonics) equipped with a high-frequency ultrasound probe (RMV-707B). Left ventricular (LV) dimensions, end-diastolic interventricular septum thickness (IVS;d), end-diastolic LV posterior wall thickness (LVPW;d), LV fractional shortening (FS), LV mass, and LV ejection fraction (EF) were measured from LV M-Mode images.

Histology and Various Staining

Heart paraffin sections were processed as previously described (6). Sirius Red staining was used for collagen deposition (7), and myocyte cross-sectional areas were determined using FITC-conjugated wheat germ agglutinin (WGA; Alexa Fluor 488 conjugate; Molecular Probes/Invitrogen). Immunohistochemical (IHC) staining with anti–8-hydroxyguanosine (8-OHdG; 1:100 dilution; Abcam, Cambridge, MA) and immunofluorescent staining with anti-Nrf2 (1:100 dilution; Santa Cruz Biotechnology, Dallas, TX) were also performed (6).

Western Blot Analysis

Western blotting was done as previously described (8–10) using primary antibodies for transforming growth factor-β1 (TGF-β1; 1:1,000 dilution; Cell Signaling Technology, Beverly, MA), connective tissue growth factor (CTGF; 1:500 dilution), followed by anti-IgG horseradish peroxidase–conjugated secondary antibody and GAPDH (1:3,000 dilution) as an internal control (all from Santa Cruz Biotechnology). MT expression was detected with a modified Western blot protocol, as previously described using antibody against MT (1:1,500 dilution; DakoCytomation, Carpinteria, CA).

Quantitative Real-Time PCR

Gene expression was examined by quantitative real-time PCR (qRT-PCR) as previously described (10) using the following primers: Nrf2 (Mm00477784), NQO1 (Mm01253561), HO-1 (Mm00516005), atrial natriuretic peptide (ANP; Mm01255747), β-myosin heavy chain (β-MHC; Mm01319006), monocyte chemoattractant protein-1 (MCP-1; Mm00441242), interleukin-6 (IL-6; Mm00446190), MT1 (Mm00496660), and GAPDH (Mm99999915) (Life Technologies, Grand Island, NY).

Determination of Lipid Peroxidation

Heart lipid peroxidation was examined using thiobarbituric acid–reactive substances assay according to the formation of malondialdehyde (MDA) during acid hydrolysis of the lipid peroxide compound, as previously described (8).

Statistical Analyses

Data were presented as mean $\pm$ SD (n = 6). Statistical analysis was calculated using one-way ANOVA with Tukey post hoc test by using Prism 5.0 (GraphPad Software, San Diego, CA). A P value <0.05 was considered statistically significant.

RESULTS

Diabetes-Induced Cardiac Dysfunction and Structural Changes Were Exacerbated in Nrf2-KO Mice and Prevented by SFN Treatment via Nrf2 Activation in WT Mice, but Not in Nrf2-KO Mice

T2DM was induced in Nrf2-KO and WT (C57BL/6J) mice (Supplementary Fig. 1*B*). Body weight and blood glucose after 3-h fasting were significantly increased in both diabetic WT and Nrf2-KO mice, which were not affected by SFN treatment (Supplementary Fig. 1*C* and *D*).

Diabetes-induced cardiac dysfunction was reflected by decreased FS and EF and increased ventricular diastolic and systolic dimension in the WT mice. These changes were more significantly observed in the Nrf2-KO mice compared with WT mice, whereas treatment with SFN significantly prevented cardiac dysfunction in WT group, but not in Nrf2-KO group (Table 1).

Lack of cardiac *Nrf2* gene in Nrf2-KO mice was confirmed by undetectable mRNA expression compared with *Nrf2* expression in WT mice (Fig. 1*A*). Nuclear Nrf2 accumulation was increased in the SFN group, decreased in the DM group, and only slightly decreased in DM/SFN group (Fig. 1*B*). Consistent with increased LV dimension noted on transthoracic echocardiography, the gross

cardiac dimensions were increased in DM groups (Fig. 1*C*). Cardiomyocyte size was increased by analysis of myocyte area via WGA staining (Fig. 1*D* and *E*). Morphological hypertrophy of the heart was further confirmed by increased expression of the molecular hypertrophy markers *ANP* and *β-MHC* mRNA (Fig. 1*F* and *G*). All of these hypertrophic indices were more significantly increased in diabetic Nrf2-KO mice than diabetic WT mice and almost completely inhibited by SFN treatment in WT mice, but not in Nrf2-KO mice (Fig. 1*C–G*).

The cardiac fibrotic response, defined by increased collagen accumulation (Fig. 2*A* and *B*) and protein expression of fibrotic mediators CTGF (Fig. 2*C* and *D*) and TGF-β1 (Fig. 2*C* and *E*), was evident in the WT diabetic group and further elevated in the Nrf2-KO diabetic group. SFN treatment prevented diabetes-induced fibrotic responses only in diabetic WT mice. Cardiac mRNA expression of inflammatory cytokines *IL-6* and *MCP-1* increased in diabetic WT and further increased in Nrf2-KO diabetic mice. SFN treatment prevented diabetes-associated inflammation completely only in diabetic WT mice (Fig. 2*F* and *G*).

Diabetes-Induced Cardiac Oxidative Stress Was Exacerbated in Nrf2-KO Mice and Prevented by SFN Treatment With Nrf2 Activation in WT Mice, but Not in Nrf2-KO Mice

Cardiac oxidative damage, defined by 8-OHdG staining (Fig. 3*A* and *B*) and lipid peroxidation with MDA assay (Fig. 3*C*), was noted in diabetic WT mice and further

Table 1—Protective effect of SFN on diabetes-induced cardiac dysfunction

	Ctrl	Ctrl/SFN	DM	DM/SFN
WT mice				
IVS;d	0.65 ± 0.04	0.68 ± 0.03	0.68 ± 0.03	0.67 ± 0.06
IVS;s	1.02 ± 0.04	1.07 ± 0.07	1.02 ± 0.09	1.03 ± 0.10
LVID;d	3.78 ± 0.08	3.73 ± 0.05	4.10 ± 0.15*	3.96 ± 0.15*
LVID;s	2.04 ± 0.1	2.01 ± 0.12	2.63 ± 007*	2.24 ± 0.18#
LVPW;d	0.88 ± 0.05	0.89 ± 0.03	0.79 ± 0.12	0.87 ± 0.14
LVPW;s	1.24 ± 0.02	1.27 ± 0.03	1.23 ± 0.09	1.27 ± 0.04
EF	76.47 ± 3.12	78.23 ± 2.49	62.71 ± 2.29*	73.51 ± 2.96#
FS	43.79 ± 3.46	46.18 ± 2.46	31.69 ± 1.40*	41.92 ± 2.53#
LV mass	88.79 ± 5.14	96.43 ± 3.9	108.15 ± 21.65	102.06 ± 12.69
LV vol;d	59.49 ± 5.17	59.43 ± 1.93	72.51 ± 8.75*	68.34 ± 5.91
LV vol;s	13.66 ± 2.03	12.98 ± 1.83	27.12 ± 1.11*	18.17 ± 2.64#
Nrf2-KO mice				
IVS;d	0.67 ± 0.04	0.66 ± 0.05	0.65 ± 0.02	0.62 ± 0.05
IVS;s	1.05 ± 0.09	1.14 ± 0.15	0.99 ± 0.13	1.01 ± 0.10
LVID;d	3.77 ± 0.05	3.76 ± 0.04	4.21 ± 0.16*	4.19 ± 0.19*
LVID;s	2.12 ± 0.09	1.99 ± 0.15	3.01 ± 0.02*	2.99 ± 0.18*
LVPW;d	0.86 ± 0.04	0.89 ± 0.07	0.92 ± 0.08	0.81 ± 0.11
LVPW;s	1.31 ± 0.03	1.30 ± 0.06	1.24 ± 0.06	1.20 ± 0.04
EF	75.67 ± 2.06	79.17 ± 4.03	53.72 ± 3.59*	54.91 ± 1.92*
FS	43.35 ± 1.21	47.19 ± 3.93	25.85 ± 2.71*	26.01 ± 1.65*
LV mass	99.39 ± 5.39	102.78 ± 5.14	127.72 ± 8.42*	126.02 ± 15.43*
LV vol;d	61.02 ± 2.04	60.39 ± 1.62	79.35 ± 9.62*	78.25 ± 8.46*
LV vol;s	15.37 ± 1.09	12.57 ± 2.42	35.34 ± 0.58*	34.97 ± 2.33*

Data are presented as means ± SD. IVS;s, end-systolic interventricular septum thickness; LVID;d, LV internal-diastolic diameter; LVID;s, LV internal-systolic diameter; LVPW;s, end-systolic LV posterior wall thickness; LV vol;d, LV end-diastolic volume; LV vol;s, LV end-systolic volume. *P < 0.05 vs. Ctrl group; #P < 0.05 vs. DM group.
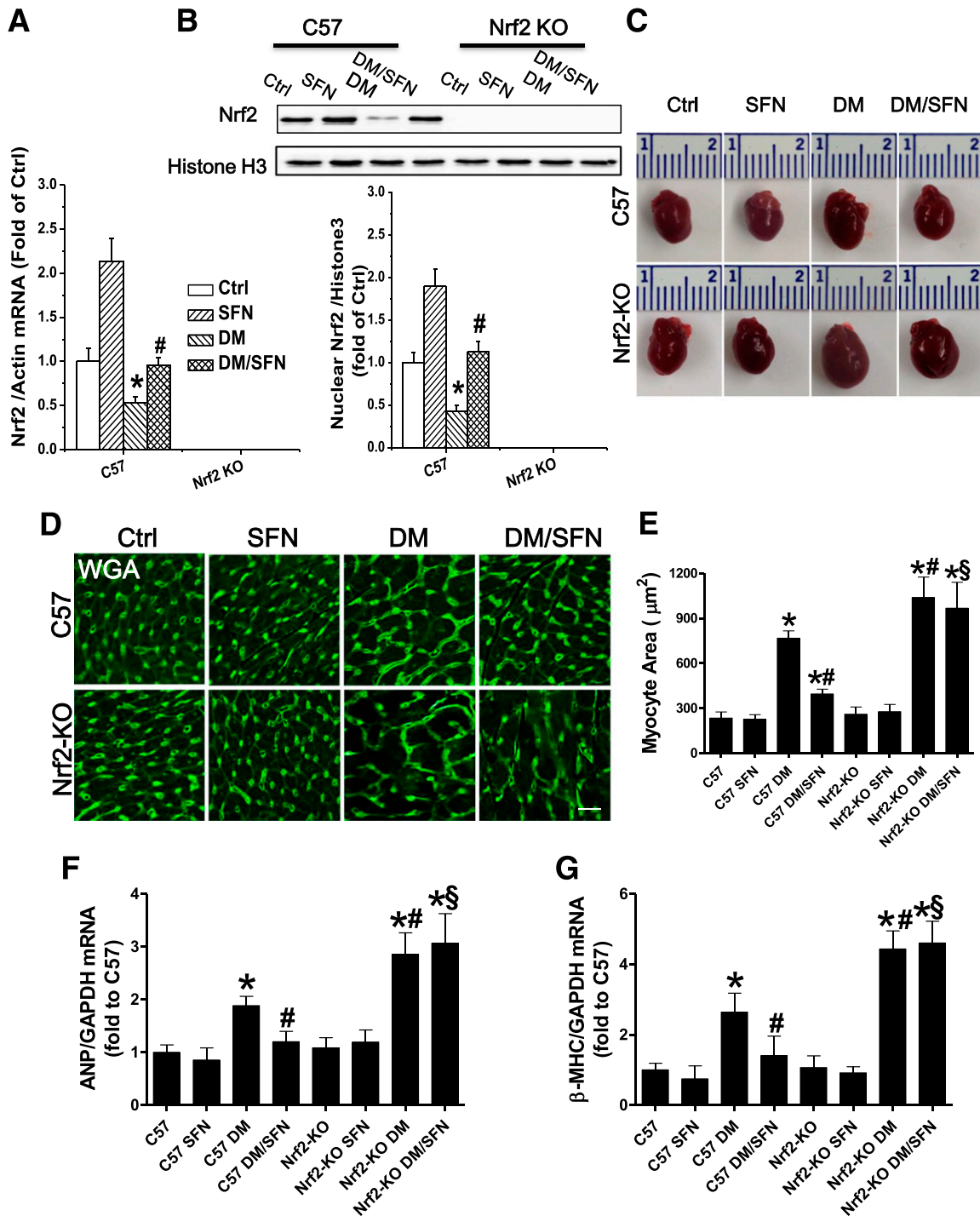
Figure 1—Nrf2-KO mice showed increased diabetes-induced cardiac hypertrophy and reduced SFN-induced cardiac protection. *A*: Nrf2 mRNA level was detected by qRT-PCR. *B*: Nuclear Nrf2 protein expression was detected by Western blot. *C*: Heart size. *D* and *E*: Cardiac tissue FITC-conjugated WGA staining and quantification of myocyte cross-sectional areas (scale bar = 25 μm). *F* and *G*: qRT-PCR analysis of hypertrophic markers *ANP* and *β-MHC* to determine mRNA expression. Data were presented as means ± SD (*n* = 6). *$P < 0.05$ vs. C57 Ctrl; #$P < 0.05$ vs. C57 DM; §$P < 0.05$ vs. C57 DM/SFN.

increased in diabetic Nrf2-KO mice. SFN treatment completely prevented these effects only in diabetic WT mice.

Immunofluorescent staining of Nrf2 (Fig. 3D) showed its expression in both cytosolic and nuclear compartments in WT controls and much less for both locations in

diabetic group. SFN significantly increased nuclear Nrf2 contents in WT controls and also preserved its normal nuclear levels in the DM/SFN group, suggesting the potential activation of Nrf2. This was supported by increased transcriptional expression of its downstream
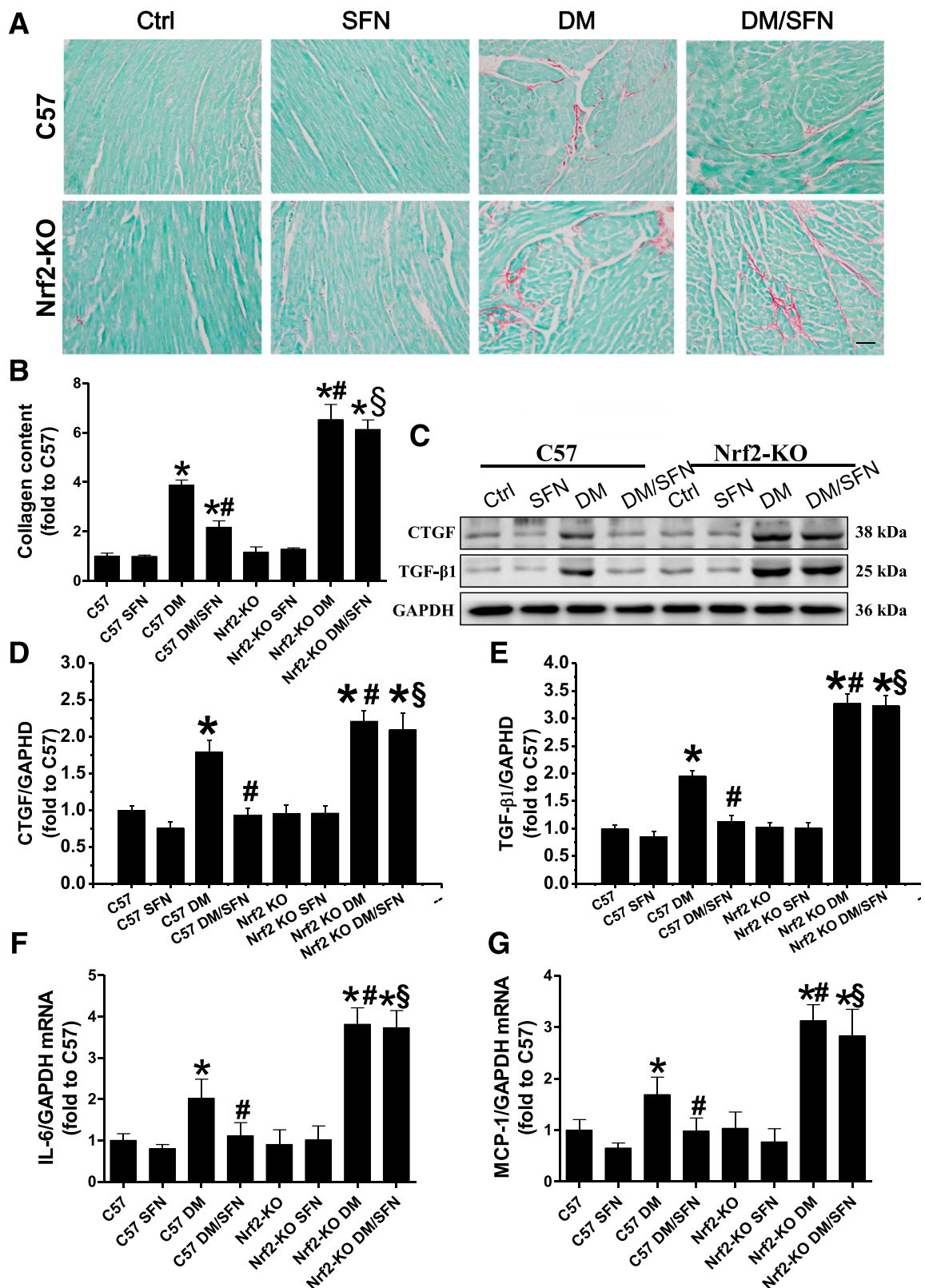
Figure 2—Nrf2-KO mice showed increased diabetes-induced cardiac fibrosis and reduced SFN-mediated cardiac protection. *A*: Cardiac fibrosis, determined by Sirius Red staining of collagen accumulation (collagen is red; scale bar = 50 μm). *B*: Quantitative analysis of Sirius Red staining for collagen accumulation. *C–E*: Protein expression of CTGF and TGF-β1 by Western blot. *F* and *G*: Cardiac inflammation, measured by mRNA expression of *IL-6* and *MCP-1* by qRT-PCR. Data were presented as means ± SD (*n* = 6). *$P < 0.05$ vs. C57; #$P < 0.05$ vs. C57 DM; §$P < 0.05$ vs. C57 DM/SFN.
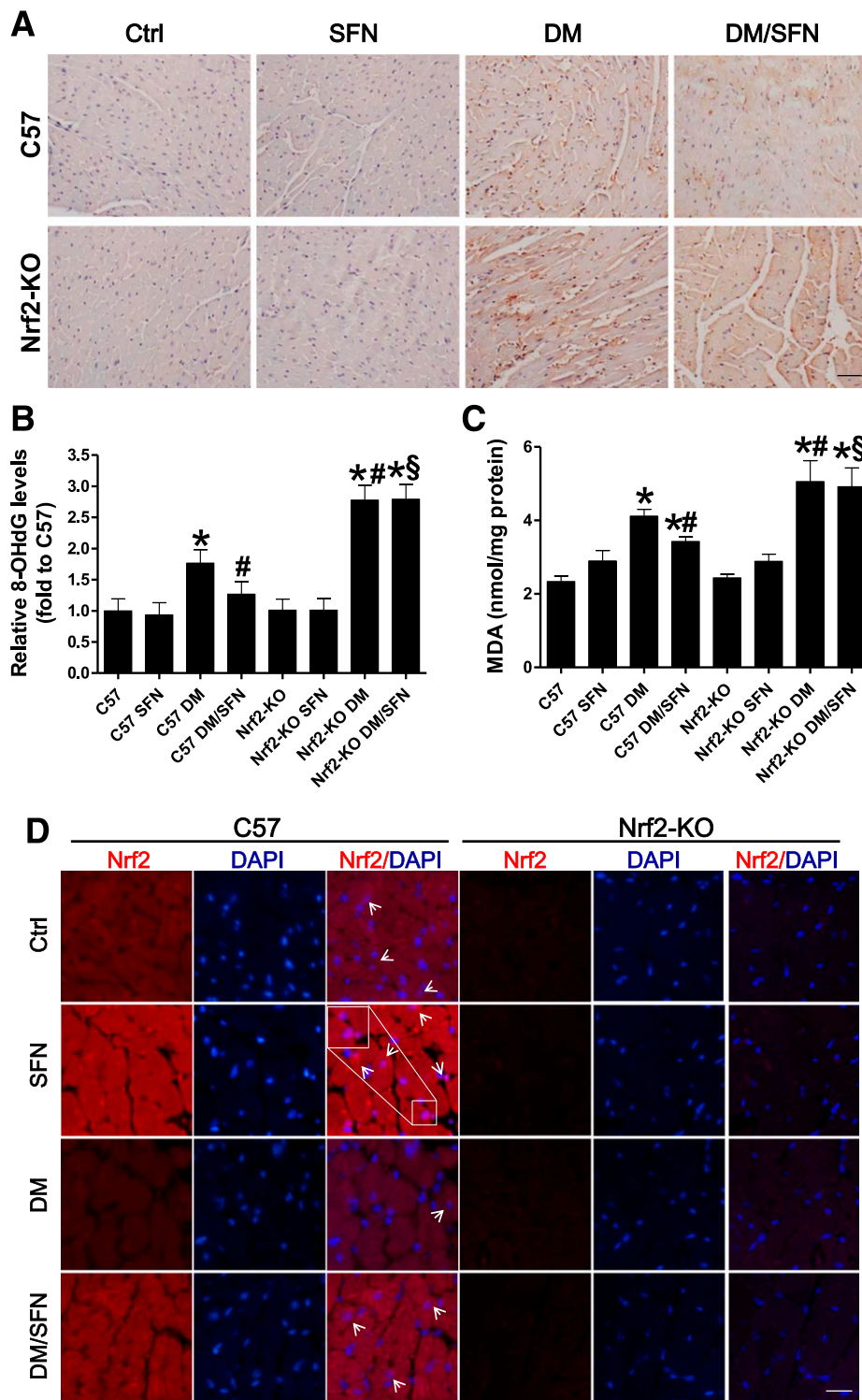
Figure 3—SFN completely abolished induced Nrf2 expression and function as well as MT expression. Cardiac oxidative damage, tested by IHC staining for 8-OHdG (A; brown considered positive staining; scale bar = 50 μm) followed by a quantitative analysis of the IHC stains (B) and lipid peroxidation with MDA assay (C). Activation of Nrf2, reflected by its nucleus accumulation (indicated by white arrows) determined by immunofluorescent staining with Nrf2 antibody (red) and nuclear staining with DAPI (blue) on cardiac tissue sections by fluorescence microscope (D) (scale bar = 25 μm) and mRNA expression of Nrf2 downstream genes HO-1 and NQO1 (E). F: MT expression measured by quantitative PCR and Western blots for its mRNA and protein levels, respectively. Data were presented as means ± SD (n = 6). *P < 0.05 vs. C57; #P < 0.05 vs. C57 DM; §P < 0.05 vs. C57 DM/SFN.
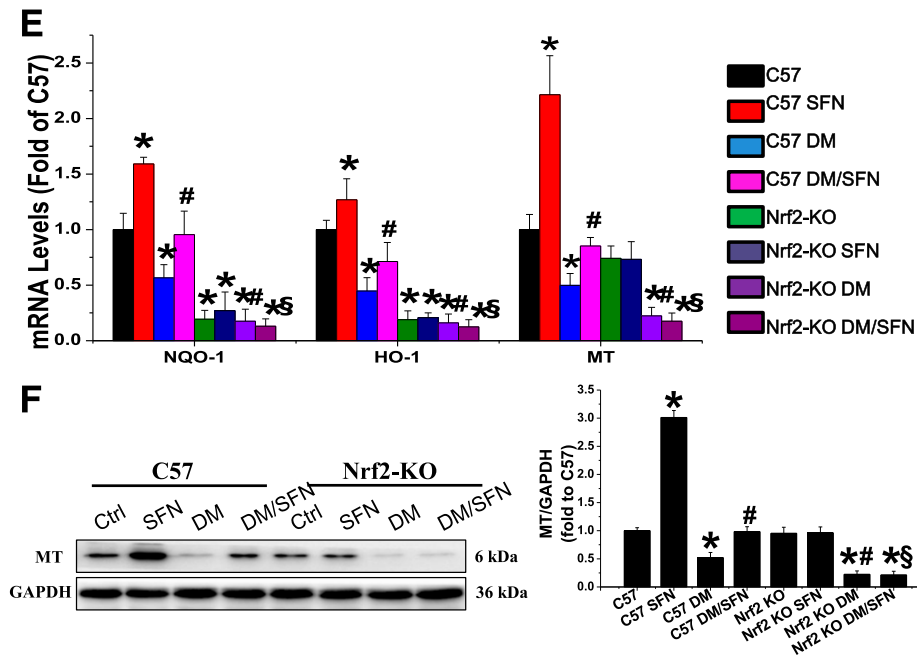
Figure 3—*Continued.*

genes *NQO1* and *HO-1* in SFN-treated WT control and diabetic groups (Fig. 3*E* and *F*). We also found that upregulated Nrf2 transcriptional function was accompanied with increased expression of MT mRNA (Fig. 3*E*) and protein (Fig. 3*F*). SFN did not stimulate Nrf2 expression and nuclear accumulation as well as its downstream genes, including MT, in Nrf2-KO mice (Fig. 3*D–F*).

Diabetes-Induced Cardiac Damages Were Exacerbated in MT-KO Diabetic Mice and Prevented by SFN in WT Diabetic Mice and Partially or Completely in MT-KO Diabetic Mice

To determine if MT plays an important role in SFN cardioprotection from diabetes, diabetic and nondiabetic MT-KO and WT (129S1) mice were treated and analyzed by the same protocol (Supplementary Fig. 2*A*). Both MT-KO and WT diabetic mice exhibited significantly increased body weight and fasting blood glucose, effects that SFN did not prevent (Supplementary Fig. 2*B* and *C*). *MT*1 mRNA and MT protein expressions were not detectable in MT-KO mice regardless of SFN treatment. However, *MT1* mRNA and protein expression decreased in DM WT mice and increased in SFN versus healthy control and DM/SFN versus DM groups, respectively (Fig. 4*A* and *B*).

The increased gross heart size (Fig. 4*C*), myocardial cell size (Fig. 4*D*), and mRNA expression of hypertrophic markers *ANP* and *β-MHC* genes (Fig. 4*E* and *F*) were consistent with DM-induced cardiac hypertrophy. These effects were more evident in MT-KO mice than WT mice, and SFN prevented cardiac hypertrophy significantly in WT mice and partially in MT-KO mice.

Diabetes-induced cardiac fibrosis (Sirius Red staining for collagen accumulation [Fig. 5*A* and *B*] and Western blotting of CTGF and TGF-β expression [Fig. 5*C–E*]) and inflammation (*IL-6* and *MCP-1* mRNA expression [Fig. 5*F* and *G*]) were also more evident in MT-KO mice than WT mice. However, SFN prevented these effects significantly in WT diabetic mice and only for inflammation and collagen accumulation in MT-KO diabetic mice, but not for CTGF and TGF-β expression.

Cardiac oxidative damage (8-OHdG) (Fig. 6*A* and *B*) and lipid peroxidation (MDA) (Fig. 6*C*) were significantly induced in both diabetic WT and MT-KO mice, particularly severely in the latter. Deletion of *MT* gene did not significantly reduce SFN cardioprotection from diabetes. This is the first evidence that deletion of the *MT* gene exacerbates diabetes-induced cardiac remodeling and other abnormal changes, but MT is not required for SFN-mediated T2DM cardioprotection.

The association of Nrf2 and MT was examined in MT-KO and their WT mice treated with or without SFN. Immunofluorescent staining showed that diabetes decreased Nrf2 expression and nuclear accumulation in both WT and MT-KO mice, whereas SFN treatment increased Nrf2 expression and nuclear accumulation under normal conditions and reversed diabetes-decreased Nrf2 expression and nuclear accumulation in both MT-KO and WT diabetic mice (Fig. 6*D*). Nrf2 expression and activation were further confirmed with its mRNA expression by real-time PCR assay (Fig. 7*A*), its nuclear accumulation by Western blotting of nuclear proteins (Fig. 7*B*), as well as Nrf2 downstream genes *NQO1* and *HO-1* mRNA expressions by real-time PCR assay (Fig. 7*C* and *D*),
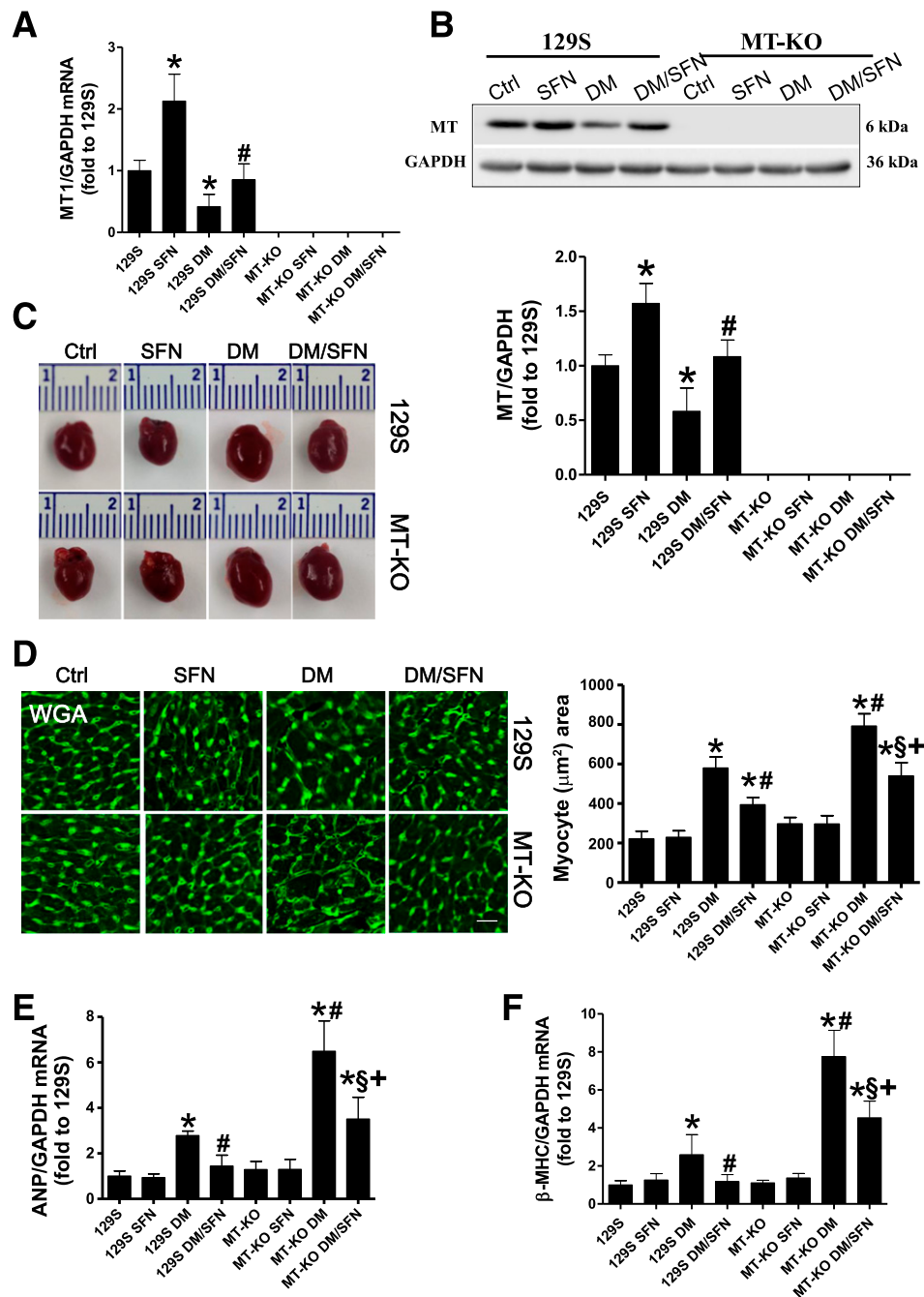
Figure 4—MT-KO mice showed increased diabetes-induced cardiac hypertrophy and preserved SFN-induced cardiac protection. *A* and *B*: MT mRNA and protein expression, evaluated by quantitative PCR and Western blot. *C*: Heart size. *D*: WGA-FITC staining in cardiac tissue sections and the quantification of myocyte cross-sectional areas (scale bar = 25 μm). *E* and *F*: Cardiac hypertrophy, detected with hypertrophic markers *ANP* and *β-MHC* with qRT-PCR. *$P < 0.05$ vs. 129S; #$P < 0.05$ vs. 129S DM; §$P < 0.05$ vs. 129S DM/SFN; +$P < 0.05$ vs. MT-KO DM.

suggesting that SFN-induced Nrf2 activation was predominantly MT independent.

DISCUSSION

Although our previous studies have shown the association of SFN-induced cardiac Nrf2 activation during the prevention of DCM in T1DM (6) and T2DM (7),

the current study confirms that Nrf2 plays a requisite role for SFN-mediated cardioprotection against T2DM because of the lack of DCM prevention by SFN in Nrf2-KO mice.

In the current study, we also demonstrated, for the first time, significant cardiac hypertrophy (Fig. 4*D*–*F*), fibrosis (Fig. 5*A*–*E*), inflammation (Fig. 5*F* and *G*), and oxidative damage (Fig. 6*A*–*C*) in MT-KO DM mice
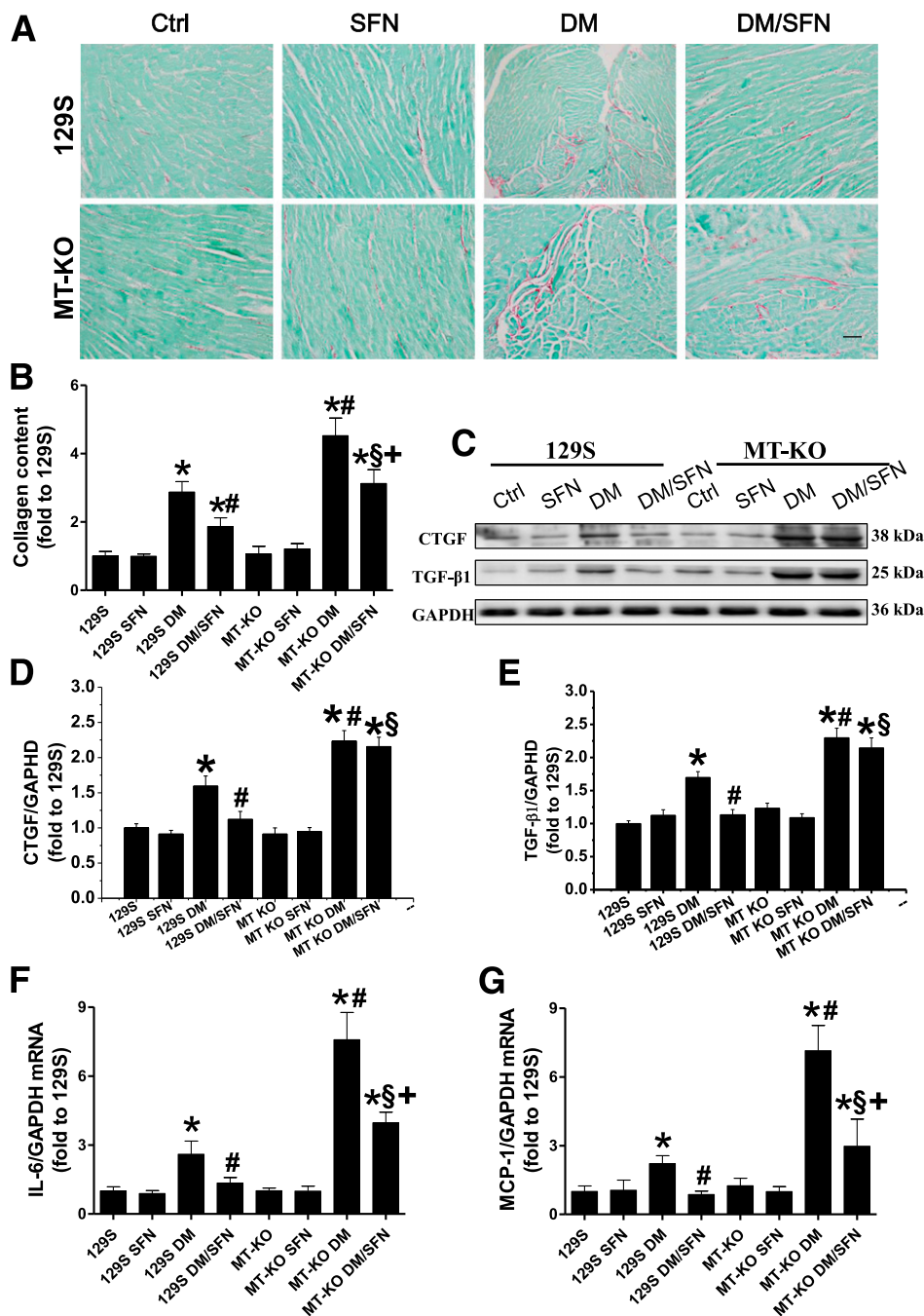
Figure 5—MT-KO mice showed increased diabetes-induced cardiac fibrosis and preserved SFN-induced cardiac protection. *A* and *B*: Cardiac fibrotic response, examined by Sirius Red staining of collagen (collagen is red; scale bar = 50 μm) and quantitative analysis. *C–E*: Protein expression of CTGF and TGF-β1 with Western blot. *F* and *G*: qRT-PCR analysis for the inflammatory factors *IL-6* and *MCP-1* to determine mRNA expression. Data were presented as means ± SD ($n = 6$). *$P < 0.05$ vs. 129S; #$P < 0.05$ vs. 129S DM; §$P < 0.05$ vs. 129S DM/SFN; +$P < 0.05$ vs. MT-KO DM.

compared with WT diabetic mice, suggesting that the basal level of MT is important for the attenuation of diabetes-induced cardiac side effects. In the literature, there is a small number of studies on diabetes using MT-KO mice (2,20). Tachibana et al. (20) have firstly shown the exacerbation of diabetic nephropathy in MT-KO mice compared with WT diabetic mice, which was supported by our recent study on diabetic nephropathy (2).

However, there was no information for the effect of the *MT* gene deletion on the heart under diabetic conditions. Furthermore, using mice overexpressing the MT gene specifically in cardiomyocytes, we have shown the significant prevention of the diabetes-induced pathological damage and function alterations (8–10).

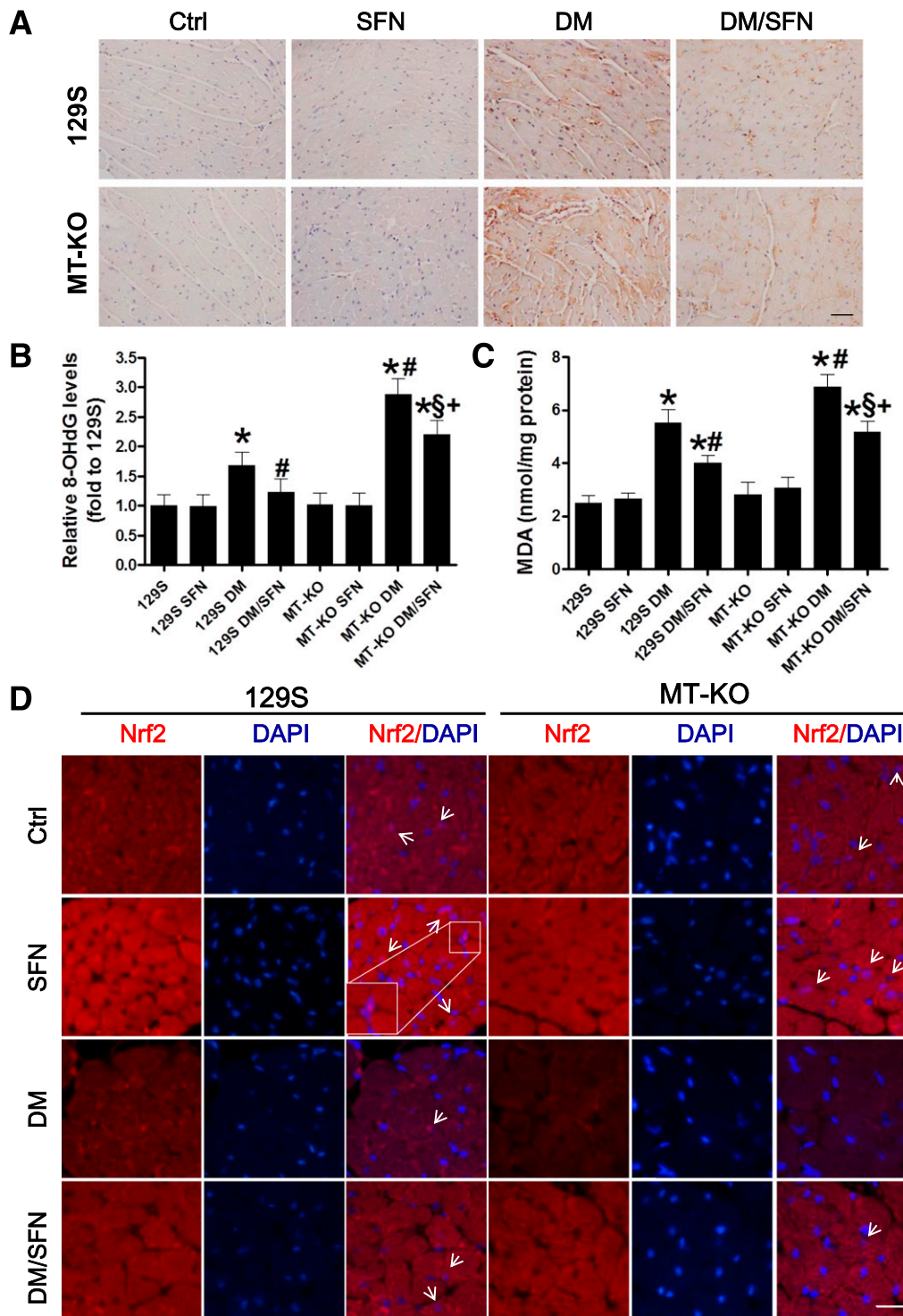Previous studies clearly indicate that both Nrf2 and MT play important roles in the prevention of DCM, but

Figure 6—SFN-induced Nrf2 expression was MT independent. Cardiac oxidative damage, detected by IHC staining with an anti–8-OHdG antibody (A; brown considered positive staining; scale bar = 50 μm) and quantitative analysis of IHC staining (B) and lipid peroxidation with MDA assay (C). D: Immunofluorescent staining with Nrf2 antibody (red) and nuclear staining with DAPI (blue) on cardiac tissue sections by fluorescence microscope (scale bar = 25 μm). White arrows indicate Nrf2 localized in the nucleus. Data were presented as means ± SD (n = 6). *$P < 0.05$ vs. 129S; #$P < 0.05$ vs. 129S DM; §$P < 0.05$ vs. 129S DM/SFN; +$P < 0.05$ vs. MT-KO DM.

there are few studies that investigated both Nrf2 and MT in the same study. For the induction of MT, most studies used zinc (9,21–23), whereas studies on the induction of Nrf2 used SFN in different conditions (6,14,18,24,25). In fact, both Zn and SFN were able to induce MT and Nrf2 (2,6,12,13,26–29). These findings prompted us to ask whether MT functioned as one of Nrf2's downstream targets to play a protective role. In this study, we
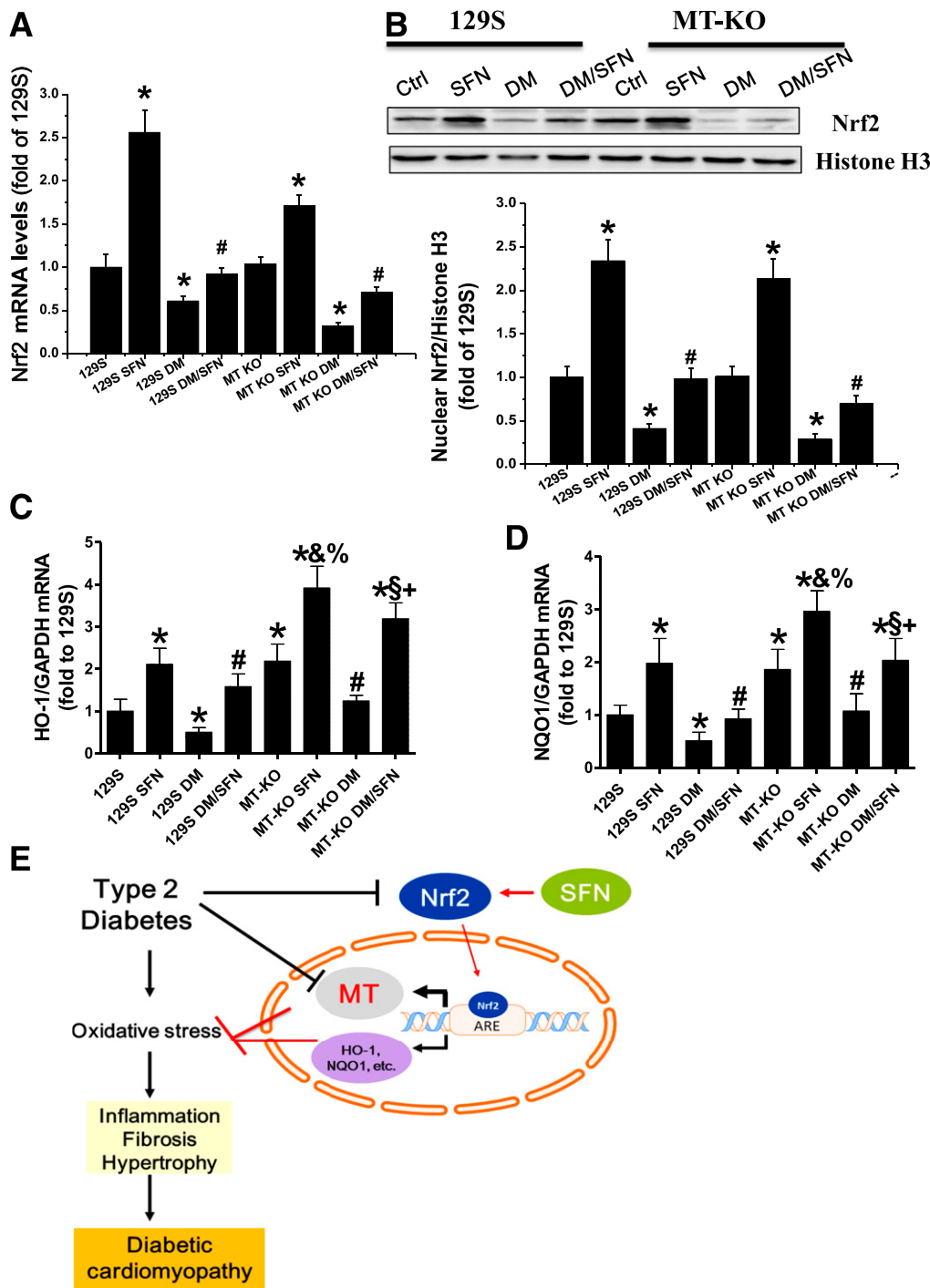
Figure 7—SFN-induced Nrf2 downstream gene expression was MT independent. *A*: The mRNA levels of Nrf2 were detected by qRT-PCR. *B*: The activation of Nrf2, which was reflected by its nuclear accumulation, was quantified by Western blot of the cardiac nucleus protein. *C* and *D*: *HO-1* and *NQO1* mRNA expression. Data were presented as means $\pm$ SD (n = 6). *E*: Schematic illustration for SFN protection against type 2 DCM. T2DM induces cardiac oxidative stress, inflammation, and fibrosis, leading from myocardial remodeling and dysfunction to development of DCM. SFN-induced cardiac protection from diabetes via upregulating Nrf2 expression and function, including Nrf2 downstream MT, NQO1, and HO-1 expression. MT, as one of the major Nrf2 downstream targets, plays an important role in the protection by SFN-induced Nrf2 pathway against type 2 DCM. *$P < 0.05$ vs. 129S; #$P < 0.05$ vs. 129S DM; §$P < 0.05$ vs. 129S DM/SFN; %$P < 0.05$ vs. MT-KO; +$P < 0.05$ vs. MT-KO DM; &$P < 0.05$ vs. 129S SFN.

demonstrated for the first time that: *1*): cardiac *MT1* mRNA and MT protein levels were in parallel with Nrf2 expression in WT mice (Fig. 3*E* and *F*); *2*) SFN induces

cardiac expression of MT at both mRNA and protein levels in the WT control mice, but not in Nrf2-KO control mice (Fig. 3*E* and *F*); and *3*) SFN can reserve the almost-

normal levels of cardiac MT mRNA and protein in the WT diabetic group, but not in Nrf2-KO diabetic mice (Fig. 3E and F), suggesting the Nrf2-dependent induction of MT by SFN. Our in vivo finding supports previous in vitro studies that have implicated MT as a downstream target of Nrf2 in cultured cells (30,31). For instance, exposure of bovine aortic endothelial cells to cadmium results in modification of Keap1, leading to Nrf2 activation and thereby upregulating both of its typical downstream proteins and MT-1/2. Chromatin immunoprecipitation assays show that Nrf2 is recruited to the antioxidant response element of the promoter region of the bovine MT-2 gene in the presence of cadmium.

Considering that both Nrf2 and MT are oxidation-responsive genes, their expressions, in a general view, should be increased as a compensative response when there is oxidative stress. However, in this study, we showed decrease in both Nrf2 and MT expression in the diabetic group. This may be because the experimental terminating time is relatively late in diabetes (6 months of diabetes). Cardiac Nrf2 expression was noted to be increased in the heart of diabetic mice at 2 weeks (32) and even 2 or 3 months (6,33), but significantly decreased in the hearts of diabetic mice at 5 or 6 months (6,33) after the onset of DM. These findings from animal models are also in a line with clinical observations: a downregulation of Nrf2 expression (mRNA and/or protein) in the failing hearts of patients with diabetes (33), peripheral blood mononuclear cells obtained from patients with prediabetes and diabetes (34,35), and skin tissue in patients with diabetes (36). Therefore, Nrf2 might be compensatively trying to remain functionally overcoming diabetic damage at the early stage, but showed a decreased rate at the late stage of diabetes because of certain mechanisms. Regarding the mechanisms by which diabetes downregulates Nrf2 expression and function at the late stage, it remains unclear based on the current study. However, it may be related to the increased proteasome activity in the diabetic tissues or cells. In diabetic rats and mice, the proteasome activity increased in skeletal muscle or heart (37,38) and kidney (39,40). Furthermore, inhibition of proteasome activity significantly reversed diabetic downregulation of Nrf2 expression and function (39,40), suggesting the negative role of diabetes-increased proteasome activity at the late stage in diabetic downregulation of Nrf2 and, consequently, MT mRNA and protein expressions.

Another unexpected finding in the current study is that although MT, as a potent antioxidant, plays an important role in the protection from diabetic complications and is one of Nrf2 downstream targets, it was not required for SFN-induced protection from DCM via upregulation of Nrf2 function. We found that in MT-KO mice, SFN continued significantly upregulating Nrf2 function and protecting the heart from diabetes for most measurements (Figs. 4–7 and Supplementary Table 1), except for CTGF and TGF-β expressions (Fig. 5D and E

and Supplementary Table 1). Thus, MT played an important, although partial, role in SFN's protection from diabetic nephropathy because SFN's renal protection from diabetes was less in MT-KO diabetic mice than that in WT diabetic mice (2). Although we have yet to define the mechanisms for differential sensitivity and/or protective effects between the heart and kidney, we speculate that SFN-induced Nrf2 activation subsequently induces MT gene expression along with other Nrf2 downstream antioxidants such as HO-1 and NQO1, as illustrated in Fig. 7E. Therefore, how and which downstream components play roles may be different among the organs, and models have yet to be determined.

HO-1, for instance, is inducible by many factors, including heavy metals and reactive oxygen species and catalyzes the first and rate-controlling step of the degradation of heme into ferrous iron, carbon monoxide, and biliverdin that is subsequently converted into bilirubin (41). Emerging evidence indicates that HO-1, along with its reaction products bilirubin and carbon monoxide, plays an important role in the protection of cardiovascular system from a wide range of oxidative stresses, including diabetes (41). We have demonstrated that diabetes downregulated cardiac Nrf2 expression and function at its late stage with significant decrease in HO-1 induction, and SFN preserved Nrf2 and HO-1 function with a significant prevention of DCM (6); however, in vitro silence of Nrf2 resulted in downregulation of HO-1 expression along with the increased cardiac cell's sensitivity to high levels of glucose-induced damage (6). Other in vitro and in vivo studies also showed the important protection by activating HO-1 via Nrf2 from cardiac damage induced by diabetic and nondiabetic conditions (42,43). These studies suggest that like MT, HO-1 may also play an important role in SFN-induced cardiac protection from diabetes. This notion is supported by our finding in this study that cardiac expression of HO-1 as well as NQO-1 mRNA in the MT-KO mice was significantly increased both in controls (about twofold vs. WT control) and SFN group (about twofold vs. MT-KO control and fourfold vs. WT control). This suggests that in the MT-KO mice, HO-1 as well as NQO-1 and other Nrf2-downstream antioxidants compensatively are upregulated in the heart to maintain the normal antioxidative defense; therefore, SFN continues inducing sufficient cardiac protection from diabetes.

Except for the Nrf2-mediated mechanism discussed above, whether there are other mechanisms that also play certain roles in the prevention of DCM by SFN is worthy of discussion. Our recent study showed a very mild reduction of glucose level in the T2DM mice treated with SFN (273.67 ± 34.20) compared with T2DM mice (324.67 ± 51.07) (7); however, under the same experimental conditions in this study, we did not see the significant difference between T2DM and T2DM/SFN in term of glucose levels (Supplementary Fig. 1D). This discrepancy is considered predominantly because of the variation among animal experiments. For instance, in the

previous study in which both self-bred and The Jackson Laboratory–purchased mice were used, both animals in the T2DM and T2DM/SFN groups showed relatively big variations of fasting blood glucose levels (DM: 51.7 mg/dL, ~15.7% of mean; DM/SFN: 34.2 mg/dL, ~12.5% of mean). In contrast, in the current study, for which both C57BL/6J and Nrf2-KO mice were purchased from The Jackson Laboratory, both animals in the T2DM and T2DM/SFN groups showed small variations: ~9% (284.0 ± 25.5) in the T2DM and 5% (277.5 ± 14.4) in the T2DM/SFN groups, respectively. Therefore, if considering the big variation of T2DM mice in the previous study, there was no significant reductive effect of SFN on blood glucose. In the literature, other studies also showed significant prevention by SFN of diabetes-induced various organ damage, but did not exhibit a significant hypoglycemic effect of SFN (6,18,44). These results thus suggested that SFN prevents DCM or other diabetic complications predominantly independent of its hypoglycemic effect. Although we did not directly measure blood pressure in the current study, we have demonstrated, in the same animal model, no significant influence on the blood pressure (7). We have reported the prevention by SFN from diabetic nephropathy in the same model (2); however, whether prevention of diabetic nephropathy by SFN results in the prevention of DCM or prevention of DCM by SFN leads to the prevention of the kidney remains unclear, which should be explored in the future with specific organ transgenic mouse models.

In summary, the current study provides the first direct evidence, to our knowledge, of the pivotal role of Nrf2 in SFN protection against T2DM-induced DCM. Because Nrf2 as a nuclear transcription factor cannot directly prevent oxidative damage, there must be Nrf2 downstream genes in SFN-induced Nrf2-mediated protection from diabetes. In this study, we show that SFN induced both Nrf2 and MT expression in the heart, but MT expression induced by SFN is Nrf2 dependent, whereas SFN-induced Nrf2 expression is MT independent. Furthermore, *MT* gene deletion did not significantly ameliorate SFN's cardiac protection from diabetes, which is predominantly because SFN-activated Nrf2 function can also upregulate other important antioxidative components such as HO-1 (Fig. 7*E*). This study has significant clinical relevance because of the association of *Nrf2* and *MT* gene polymorphisms for several diseases, including cardiovascular diseases (45,46). Once we refine the relationship of Nrf2 with MT in diabetes, we can explore strategies that upregulate MT and/or Nrf2 for patients with genetic polymorphisms, such as via SFN and/or zinc to induce cardiac protection.

References

1. Chen J, Zhang Z, Cai L. Diabetic cardiomyopathy and its prevention by nrf2: current status. Diabetes Metab J 2014;38:337–345
2. Wu H, Kong L, Cheng Y, et al. Metallothionein plays a prominent role in the prevention of diabetic nephropathy by sulforaphane via up-regulation of Nrf2. Free Radic Biol Med 2015;89:431–442
3. Giacco F, Brownlee M. Oxidative stress and diabetic complications. Circ Res 2010;107:1058–1070
4. Cai L, Kang YJ. Oxidative stress and diabetic cardiomyopathy: a brief review. Cardiovasc Toxicol 2001;1:181–193
5. Nguyen T, Nioi P, Pickett CB. The Nrf2-antioxidant response element signaling pathway and its activation by oxidative stress. J Biol Chem 2009;284:13291–13295
6. Bai Y, Cui W, Xin Y, et al. Prevention by sulforaphane of diabetic cardiomyopathy is associated with up-regulation of Nrf2 expression and transcription activation. J Mol Cell Cardiol 2013;57:82–95
7. Zhang Z, Wang S, Zhou S, et al. Sulforaphane prevents the development of cardiomyopathy in type 2 diabetic mice probably by reversing oxidative stress-induced inhibition of LKB1/AMPK pathway. J Mol Cell Cardiol 2014;77:42–52
8. Cai L, Wang Y, Zhou G, et al. Attenuation by metallothionein of early cardiac cell death via suppression of mitochondrial oxidative stress results in a prevention of diabetic cardiomyopathy. J Am Coll Cardiol 2006;48:1688–1697
9. Wang J, Song Y, Elsherif L, et al. Cardiac metallothionein induction plays the major role in the prevention of diabetic cardiomyopathy by zinc supplementation. Circulation 2006;113:544–554
10. Wang Y, Feng W, Xue W, et al. Inactivation of GSK-3beta by metallothionein prevents diabetes-related changes in cardiac energy metabolism, inflammation, nitrosative damage, and remodeling. Diabetes 2009;58:1391–1402
11. Tang Y, Yang Q, Lu J, et al. Zinc supplementation partially prevents renal pathological changes in diabetic rats. J Nutr Biochem 2010;21:237–246
12. Wang W, He Y, Yu G, et al. Sulforaphane protects the liver against CdSe quantum dot-induced cytotoxicity. PLoS One 2015;10:e0138771
13. Hu R, Hebbar V, Kim BR, et al. In vivo pharmacokinetics and regulation of gene expression profiles by isothiocyanate sulforaphane in the rat. J Pharmacol Exp Ther 2004;310:263–271
14. Wang Y, Zhang Z, Guo W, et al. Sulforaphane reduction of testicular apoptotic cell death in diabetic mice is associated with the upregulation of Nrf2 expression and function. Am J Physiol Endocrinol Metab 2014;307:E14–E23
15. Vermeulen M, Klöpping-Ketelaars IW, van den Berg R, Vaes WH. Bioavailability and kinetics of sulforaphane in humans after consumption of cooked versus raw broccoli. J Agric Food Chem 2008;56:10505–10509
16. Hanlon N, Coldham N, Gielbert A, et al. Absolute bioavailability and dose-dependent pharmacokinetic behaviour of dietary doses of the chemopreventive isothiocyanate sulforaphane in rat. Br J Nutr 2008;99:559–564
17. Guerrero-Beltrán CE, Calderón-Oliver M, Pedraza-Chaverri J, Chirino YI. Protective effect of sulforaphane against oxidative stress: recent advances. Exp Toxicol Pathol 2012;64:503–508

18.   Cui W, Bai Y, Miao X, et al. Prevention of diabetic nephropathy by sulforaphane: possible role of nrf2 upregulation and activation. Oxid Med Cell Longev 2012;2012:821936

19.   Jiang X, Bai Y, Zhang Z, Xin Y, Cai L. Protection by sulforaphane from type 1 diabetes-induced testicular apoptosis is associated with the up-regulation of Nrf2 expression and function. Toxicol Appl Pharmacol 2014;279:198–210

20.   Tachibana H, Ogawa D, Sogawa N, et al. Metallothionein deficiency exacerbates diabetic nephropathy in streptozotocin-induced diabetic mice. Am J Physiol Renal Physiol 2014;306:F105–F115

21.   Liu F, Ma F, Kong G, Wu K, Deng Z, Wang H. Zinc supplementation alleviates diabetic peripheral neuropathy by inhibiting oxidative stress and upregulating metallothionein in peripheral nerves of diabetic rats. Biol Trace Elem Res 2014;158:211–218

22.   Ohly P, Dohle C, Abel J, Seissler J, Gleichmann H. Zinc sulphate induces metallothionein in pancreatic islets of mice and protects against diabetes induced by multiple low doses of streptozotocin. Diabetologia 2000;43:1020–1030

23.   Wang X, Li H, Fan Z, Liu Y. Effect of zinc supplementation on type 2 diabetes parameters and liver metallothionein expressions in Wistar rats. J Physiol Biochem 2012;68:563–572

24.   Jiang X, Chen J, Zhang C, et al. The protective effect of FGF21 on diabetes-induced male germ cell apoptosis is associated with up-regulated testicular AKT and AMPK/Sirt1/PGC-1α signaling. Endocrinology 2015;156:1156–1170

25.   Wang Y, Zhang Z, Sun W, et al. Sulforaphane attenuation of type 2 diabetes-induced aortic damage was associated with the upregulation of nrf2 expression and function. Oxid Med Cell Longev 2014;2014:123963

26.   Cortese MM, Suschek CV, Wetzel W, Kröncke KD, Kolb-Bachofen V. Zinc protects endothelial cells from hydrogen peroxide via Nrf2-dependent stimulation of glutathione biosynthesis. Free Radic Biol Med 2008;44:2002–2012

27.   Miao X, Wang Y, Sun J, et al. Zinc protects against diabetes-induced pathogenic changes in the aorta: roles of metallothionein and nuclear factor (erythroid-derived 2)-like 2. Cardiovasc Diabetol 2013;12:54

28.   Li B, Cui W, Tan Y, et al. Zinc is essential for the transcription function of Nrf2 in human renal tubule cells in vitro and mouse kidney in vivo under the diabetic condition. J Cell Mol Med 2014;18:895–906

29.   Maremanda KP, Khan S, Jena GB. Role of zinc supplementation in testicular and epididymal damages in diabetic rat: involvement of Nrf2, SOD1, and GPX5. Biol Trace Elem Res 2016;173:452–464

30.   Weng CJ, Chen MJ, Yeh CT, Yen GC. Hepatoprotection of quercetin against oxidative stress by induction of metallothionein expression through activating MAPK and PI3K pathways and enhancing Nrf2 DNA-binding activity. N Biotechnol 2011;28:767–777

31.   Shinkai Y, Kimura T, Itagaki A, et al. Partial contribution of the Keap1-Nrf2 system to cadmium-mediated metallothionein expression in vascular endothelial cells. Toxicol Appl Pharmacol 2016;295:37–46

32.   He X, Kan H, Cai L, Ma Q. Nrf2 is critical in defense against high glucose-induced oxidative damage in cardiomyocytes. J Mol Cell Cardiol 2009;46:47–58

33.   Tan Y, Ichikawa T, Li J, et al. Diabetic downregulation of Nrf2 activity via ERK contributes to oxidative stress-induced insulin resistance in cardiac cells in vitro and in vivo. Diabetes 2011;60:625–633

34.   Liu TS, Pei YH, Peng YP, Chen J, Jiang SS, Gong JB. Oscillating high glucose enhances oxidative stress and apoptosis in human coronary artery endothelial cells. J Endocrinol Invest 2014;37:645–651

35.   Jiménez-Osorio AS, Picazo A, González-Reyes S, Barrera-Oviedo D, Rodríguez-Arellano ME, Pedraza-Chaverri J. Nrf2 and redox status in prediabetic and diabetic patients. Int J Mol Sci 2014;15:20290–20305

36.   Lee YJ, Kwon SB, An JM, et al. Increased protein oxidation and decreased expression of nuclear factor E2-related factor 2 protein in skin tissue of patients with diabetes. Clin Exp Dermatol 2015;40:192–200

37.   Merforth S, Osmers A, Dahlmann B. Alterations of proteasome activities in skeletal muscle tissue of diabetic rats. Mol Biol Rep 1999;26:83–87

38.   Wang X, Hu Z, Hu J, Du J, Mitch WE. Insulin resistance accelerates muscle protein degradation: Activation of the ubiquitin-proteasome pathway by defects in muscle cell signaling. Endocrinology 2006;147:4160–4168

39.   Luo ZF, Qi W, Feng B, et al. Prevention of diabetic nephropathy in rats through enhanced renal antioxidative capacity by inhibition of the proteasome. Life Sci 2011;88:512–520

40.   Cui W, Li B, Bai Y, et al. Potential role for Nrf2 activation in the therapeutic effect of MG132 on diabetic nephropathy in OVE26 diabetic mice. Am J Physiol Endocrinol Metab 2013;304:E87–E99

41.   Czibik G, Derumeaux G, Sawaki D, Valen G, Motterlini R. Heme oxygenase-1: an emerging therapeutic target to curb cardiac pathology. Basic Res Cardiol 2014; 109:450

42.   Issan Y, Kornowski R, Aravot D, et al. Heme oxygenase-1 induction improves cardiac function following myocardial ischemia by reducing oxidative stress. PLoS One 2014;9:e92246

43.   Zhao Y, Zhang L, Qiao Y, et al. Heme oxygenase-1 prevents cardiac dysfunction in streptozotocin-diabetic mice by reducing inflammation, oxidative stress, apoptosis and enhancing autophagy. PLoS One 2013;8:e75927

44.   Shang G, Tang X, Gao P, et al. Sulforaphane attenuation of experimental diabetic nephropathy involves GSK-3 beta/Fyn/Nrf2 signaling pathway. J Nutr Biochem 2015;26:596–606

45.   Cho HY, Marzec J, Kleeberger SR. Functional polymorphisms in Nrf2: implications for human disease. Free Radic Biol Med 2015;88:362–372

46.   Yang L, Li H, Yu T, et al. Polymorphisms in metallothionein-1 and -2 genes associated with the risk of type 2 diabetes mellitus and its complications. Am J Physiol Endocrinol Metab 2008;294:E987–E992